

GALLOPING OF INSULATED BUNDLED OVERHEAD LINE SIMPLIFIED ANALYSIS

Hračov S. ^{*}, Macháček M. ^{}**

Abstract: *Our paper provides an analysis of the susceptibility of a particular bundled overhead line to galloping. It presents a case study of an aerial bundled cable, consisting of four conductors insulated by polyethylene, and used for low-voltage power lines. The susceptibility to loss of stability is analyzed for cable without and with simulated icing observed on similar real conductors. In the first case, the proneness to galloping was excluded based on the results of CFD simulation and the Den Hartog criterion. In latter case, the possible occurrence of galloping was confirmed. The critical wind velocity for the ice-covered cable was calculated utilizing quasi-steady theory. Finally, the amplitudes of limit cycle oscillation for supercritical wind speeds were estimated based on simplified numerical analysis.*

Keywords: Aerial bundled cable, wind effects, galloping, limit cycle oscillation.

1. Introduction

Due to the wind action, electrical overhead conductors often lose their aeroelastic stability in the form of galloping. Galloping is a low-frequency self-excited oscillation with amplitudes reaching up to several times the sag, most often in a plane perpendicular to the wind direction see Holmes (2018). Galloping generally cannot occur at conductors with symmetrical circular cross sections. However, especially in the winter ice accretion can significantly change their geometric cross-sections leading to a loss of stability and excessive amplitudes of limit cycle oscillation. According to a document by EPRI (2006), the occurrence of galloping was most often observed in mode shape with one to three loops.

In this paper, the specific insulated bundled cable with very low tension force is analyzed in terms of proneness to galloping with and without the effect of icing see Fig.1. The properties of this short-span low - voltage bundled line consisting of four main conductors are summarized in Tab. 1



Fig. 1: Bundled overhead line – axonometric view, cross-section and ice-covered cross-section.

2. Assessment of proneness to galloping

The necessary condition for the occurrence of self-excited oscillation – galloping, based on quasi-steady theory of a general profile, can be expressed by the Den Hartog criterion:

$$C_D(\alpha) + \frac{dC_L}{d\alpha}(\alpha) < 0 \quad (1)$$

^{*} Ing. Stanislav Hračov, PhD.: Institute of Theoretical and Applied Mechanics of the Czech Academy of Sciences, Prosecká 809/76; 190 00, Prague; CZ, hracov@itam.cas.cz

^{**} Ing. Michael Macháček, PhD.: Institute of Theoretical and Applied Mechanics of the Czech Academy of Sciences, Prosecká 809/76; 190 00, Prague; CZ, machacek@itam.cas.cz

where C_D and C_L represent the aerodynamic drag and lift coefficients, respectively, and α represents the angle of attack, which is defined in Fig. 2.

Parameter	Value
Horizontal distance of suspension points	21.1 m
Vertical distance of suspension points	1.55 m
Diameter of circumscribed circle of bundled line (D)	38 mm
Cross-sectional are of line	465.28 mm ²
Young's modulus (E)	57 GPa
Mass per unit length of line (with ice accretion)	1.69 kg/m (2.09 kg/m)
Horizontal component of tension force for: -5 °C (-5 °C with ice accretion)	930.3 N (1 149.5 N)

Tab. 1: Geometrical and mechanical properties of electric line (AES 4 x 120).

These aerodynamic coefficients of the cable related to various α are depicted in Fig. 2. The left part of this figure presents coefficients for the cable without ice accretion, while the right part values for the ice-covered line. The data related to the cable itself were determined by CFD simulation in Comsol MultiPhysics, while the aerodynamic coefficients for the cable with icing were adopted from Desai et al. (1995). The assessment of susceptibility to galloping was evaluated for several angles of attack by means of the Den Hartog criterion, which is also graphically represented in Fig. 2 by the black line. The results indicate that the conductor without icing is not prone to galloping, as shown in Fig. 2, where the black line is above the zero for the entire range of angles α . On the other hand, angular intervals of possible instability can be found for the iced-covered cable. The minima of the curve in Fig. 2 representing the Den Hartog criterion correspond to the angles of attack, which are related to the lowest critical wind speeds. The angles $\alpha_c = 40.0^\circ$, 179.3° and 187.5° were determined as critical from the viewpoint of the onset of galloping.

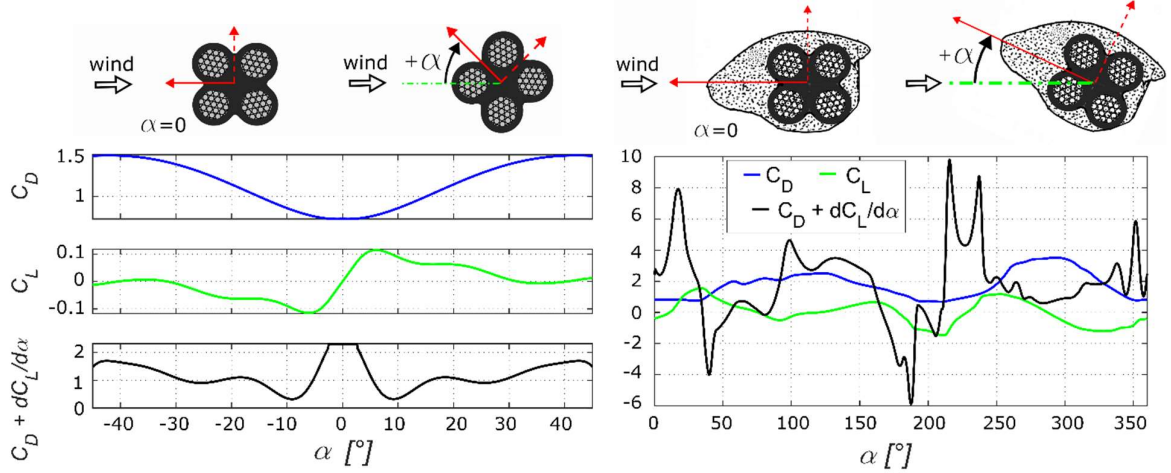


Fig. 2: Aerodynamic drag and lift coefficients, C_D and C_L , and the Den Hartog criterion for line without and with ice accretion as the functions of angle of attack α .

The estimate of critical wind speeds for the onset of self-excited transversal galloping-type oscillations of the line with icing having the cross-section related to angles α_c can be determined, as outlined in Païdoussi et al. (2010):

$$V_c(\alpha_c) = \frac{4 \cdot m \cdot \zeta \cdot 2\pi \cdot f_n}{-\left(\frac{dC_L}{d\alpha}(\alpha_c) + C_D(\alpha_c)\right) \cdot \rho \cdot D} \quad (2)$$

where m is the mass per unit length, ζ is the structural damping ratio, f_n is the natural frequency related to the in-plane natural mode i.e. mode in the plane of the static sag, ρ stands for air density and D represents the diameter of circumscribed circle of the bundled line. The wind direction is assumed horizontal.

The lowest critical wind velocity corresponds to the natural frequency of the lowest in-plane natural mode. For our bundled overhead line with ice accretion, it is the first asymmetric in-plane mode, which is depicted in Fig. 3 and corresponds to a very low frequency $f_n = 1.105$ Hz. This mode and its natural frequency were determined according to the solution in Madugula (2001), which is valid for taut cables with sag-to-span ratio 1:8 or lower. In our case, this ratio is approximately 1:17. It should be noted that due to low tension force, the natural frequency of the first symmetric in-plane mode is higher than the above stated lowest in-plane natural frequency.

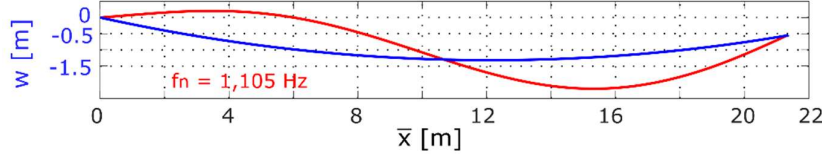


Fig. 3: Sag of the cable w , (blue curve) and the lowest natural in-plane mode (red curve).

Tab. 2 summarizes the estimated critical wind speeds for this lowest in-plane mode for three critical angles α_c . The structural damping ratio of the cable was assumed by low value $\zeta = 0.5\%$. The observed critical velocities are very low, so there is a realistic assumption of the occurrence of self-excited oscillation.

Angle of attack	$\alpha_c = 40.0^\circ$	$\alpha_c = 179.3^\circ$	$\alpha_c = 187.5^\circ$
Critical wind speed	1.59 m/s	1.85 m/s	1.08 m/s

Tab. 2: Critical wind speeds V_c for galloping of bundled overhead line with ice accretion.

3. Simplified calculation of limit cycle oscillation

The simplified calculation of the post-critical steady response is based on the assumptions of the quasi-steady theory. The harmonic oscillation of the line in the plane of the sag i.e. perpendicular to the direction of the wind in the lowest in-plane natural mode $y_n(x)$ is considered:

$$y(x, t) = A \cdot y_n(x) \cdot \sin(2\pi \cdot f_n \cdot t) \quad (3)$$

where A is amplitude of the limit cycle, x is longitudinal coordinate of the rope, $x \in (0, L)$, L is the length of the rope and t stands for time. Only in-plane motion of the cable is thus assumed, so the axial and along-wind motions as well as rotation are neglected. The Max normalization of natural mode $y_n(x)$ is used in Eq. (3). The estimation of the level of steady oscillation of the line at supercritical wind speeds is based on the assumption of equality of work, W_d , done by the structural dissipative forces, F_d , and work, W_w , done by the aerodynamic forces, F_y , acting on the oscillating line during one natural period T_n :

$$W_d = \int_0^L \int_0^{T_n} F_d(\dot{y}(x, t)) \cdot dy(x, t) \cdot dx = W_w = \int_0^L \int_0^{T_n} F_y(\dot{y}(x, t)) \cdot dy(x, t) \cdot dx \quad (4)$$

The structural damping force acting on a differential length of the cable dx at point x is considered viscous, i.e. proportional to the line velocity $\dot{y}(x, t)$:

$$F_d(\dot{y}(x, t)) \cdot dx = 4\pi \cdot f_n \cdot \zeta \cdot m \cdot \dot{y}(x, t) \cdot dx \quad (5)$$

The aerodynamic force acting on a differential length dx at point x in the direction perpendicular to the wind direction can be expressed as

$$F_y(\dot{y}(x, t)) \cdot dx = 0,5 \cdot \rho \cdot V^2 \cdot D \cdot \left(-\sec(\alpha_r(x, t)) \cdot (C_L(\alpha_c + \alpha_r(x, t)) + C_D(\alpha_c + \alpha_r(x, t)) \cdot \tan(\alpha_r(x, t))) \right) \cdot dx \quad (6)$$

where V represents the supercritical wind speed, which is considered constant along the whole cable and $\alpha_r(x, t)$ is the angle of attack of the relative wind at point x :

$$\alpha_r(x, t) = \tan^{-1}(\dot{y}(x, t)/V) \quad (7)$$

By substituting the expressions from Eq. (5) and Eq. (6) and differential $dy(x, t)$

$$dy(x, t) = 2\pi \cdot f_n \cdot A \cdot y_n(x) \cdot \cos(2\pi \cdot f_n \cdot t) \cdot dt \quad (8)$$

into Eq. (4), the supercritical wind speed V can be numerically evaluated from Eq. (4) for the chosen value of the amplitude, A . The oscillation amplitudes, as functions of wind speed for selected critical angles α_c of the analyzed line from Tab. 2, calculated according to this approach are shown graphically in Fig. 4.

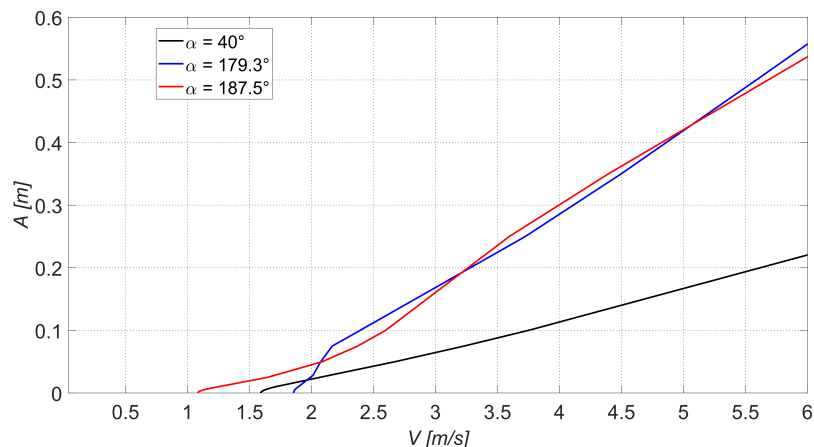


Fig. 4: Amplitude of limit cycle oscillation as function of wind speed.

4. Discussion of the results and conclusions

The numerical simulations confirmed the predicted critical wind speeds given in Tab. 2. The calculated amplitudes of the steady-state response are significant even for low wind speeds. Especially, the predicted wind effects for both angles around 180° are extreme, and the amplitudes in these cases reach almost half of the static sag for wind speed around 6 ms^{-1} . However, considering the very low static forces of this cable, it is rather impossible to assume that such amplitudes for higher wind velocities will be reached. During these predicted substantial limit-cycle oscillations, the dynamic normal forces in the cable are not negligible compared to static tensile force. This fact completely changes the prerequisite of harmonic character of the response and mainly the assumption of linearity of the mechanical system. A more sophisticated 3D FEM model, respecting the geometrical nonlinearity of the system, must be used to solve the self-excited vibration of this low-tensioned cable. The outputs from the simplified analysis with a linearized model used in this paper can serve only for the estimation of the onset of galloping-type instability.

The results of this analysis nevertheless served also for controlling, comparative purposes and calibrations during the creation of 3D FEM model. This complex model includes geometrical nonlinearity of the problem and incorporates bending stiffness, which improves the stability of calculations and the precision of results. Detailed information about the model and comparison with the results of this simplified approach are presented in another paper of authors; see Macháček and Hračov (2024).

Acknowledgement

The kind support of Czech Scientific Foundation project No. 24-13061S is gratefully acknowledged.

References

- Desai, Y. M., Yu, P., Popplewell, N. and Shah, A. H. (1995) Finite element modelling of transmission line galloping, *Computers & Structures*, 57, 3, pp. 407–420.
- EPRI (2006) *Transmission Line Reference Book - Wind Induced Conductor Motion*.
- Holmes, J. D. (2018) *Wind Loading Structures*, CRC Press, 3rd edition.
- Madugula, M. K. S. (2001) *Dynamic Response of Lattice Towers and Guyed Masts*, ASCE.
- Macháček, M. and Hračov, S. (2024) Galloping of insulated bundled overhead line – Nonlinear numerical analysis in time domain, In: *Proc. of 30th Conference Engineering mechanics 2024*. Milovy, pp. 190–193.
- Païdoussis M., Price S. J., de Langre E. (2010) *Fluid-Structure Interactions: Cross-Flow-Induced Instabilities*. Cambridge University Press.